Terahertz frequency bandpass filters

A. J. Gallant, M. A. Kaliteevski, S. Brand, D. Wood, M. Petty, R. A. Abram, and J. M. Chamberlain[a)]
Department of Physics and School of Engineering, Durham University, Durham DH1 3LE, United Kingdom

(Received 17 March 2007; accepted 1 June 2007; published online 17 July 2007)

The design, measurement, and analysis of a range of artificial materials for use at terahertz frequencies are described. The chosen structures consist of arrays of cylindrical gold-plated pillars with period comparable to the wavelength of incident radiation. An ultraviolet (UV) micromachining approach to the fabrication of these high aspect-ratio pillars is described using the negative epoxy-based resin SU8. Lattice fence structures are also realized using the same method. Terahertz (THz) frequency time domain spectroscopy is performed on these structures in the range 200 GHz to 3.0 THz and the relative transmission of the structures is determined. The pass and stop bands are observed with peak transmission of up to 97%. Finite difference time domain simulations and complex photonic band structure calculations are shown to provide good descriptions of the electromagnetic properties of the structures and are used to interpret the observed transmission spectra. © *2007 American Institute of Physics*. [DOI: 10.1063/1.2756072]

I. INTRODUCTION

The electromagnetic properties of an *artificial material*[1] can, in principle, be selected by suitable design. These properties of an artificial material, as with a naturally-occurring material, are described in terms of: refractive indices (n), permittivities (ε), and, if appropriate, permeabilities (μ). These can be arranged to be high or low, zero or even negative, and are likely to vary with frequency in the spectral region of interest. In an artificial material, the electromagnetic near field can be manipulated and exploited to realize new types of lenses, waveguides, and imaging systems. Although there is growing interest in this field in the microwave[2] and optical[3] parts of the spectrum, very little work has been reported to date in the terahertz (THz) range. This is hardly surprising, as the importance of this region (*between radio and light*) (Ref. 4) is only now emerging as new sources and functional components such as quantum cascade lasers[5] and pulsed generation techniques[6] are developed. In order to explore this region of the spectrum, devices such as THz microscopes are also being developed.[7] Although they are still in their infancy, THz microscopes have the potential to enhance further our understanding of the fundamental properties of entities from living cells, to polymers and semiconductor devices. However, for this technology to realize its potential, it is imperative that new types of lenses, probes, and filters be developed for THz operation. Artificial materials, of the type discussed in this paper, will have a role to play in the realization of such instruments.

In this article, we describe the design, measurement, and analysis of a type of artificial material for use at THz frequencies that is essentially a two-dimensional photonic crystal based on periodically spaced high aspect ratio metal pillars, which we term a *pillar forest*. It is known that such a system exhibits zero transmission of radiation with its electric field parallel to the pillars for a range of frequency from zero up to some critical frequency. Specifically, Pendry *et al.*[8,9] have shown that the critical frequency of the artificial material is the effective plasma frequency of the artificial material; hence, the material's dielectric constant is negative for lower frequencies. Pendry *et al.*[8,9] have also shown that the effective plasma frequency is dependent on the pillar diameter and spacing and can be made much lower than that of the bulk metal used for the pillars. When the radiation frequency is above the effective plasma frequency and its wavelength is comparable to the pillar spacing, the system exhibits photonic band structure effects, including transmission and stop bands. In this article, we describe the fabrication and study of pillar forest structures that have an effective plasma frequency in the THz regime and exhibit photonic band structure effects above the plasma frequency. In particular, we show that the structures can act as filters which have useful properties at THz frequencies with a relative transmission of up to 97% in the pass band.

The wavelength of the incident radiation determines the dimensional requirements of an artificial material. Micromachining techniques are ideally suited for the development of THz artificial materials (where 1 THz$\equiv$300 μm), but in the case of the pillar forests, the need to have a pillar height in excess of 1 mm to accommodate the radiation beam imposes special demands. The pillar forests were made using a novel ultraviolet (UV) exposure technique and fabrication process with SU8, a negative epoxy-based photoresist.[10] The transmission properties of these structures were measured at THz frequencies in the range 0.2–3.0 THz and interpreted using a complex band structure method and finite difference time domain (FDTD) simulations.

The paper is organized as follows: the fabrication method for realizing pillar forest and lattice fence structures is first outlined; the experimental arrangements for performing THz time domain spectroscopy are then described; the transmission results for a series of pillar forest and lattice fence structures are then given; the procedures for both

[a)]Electronic mail: martyn.chamberlain@durham.ac.uk

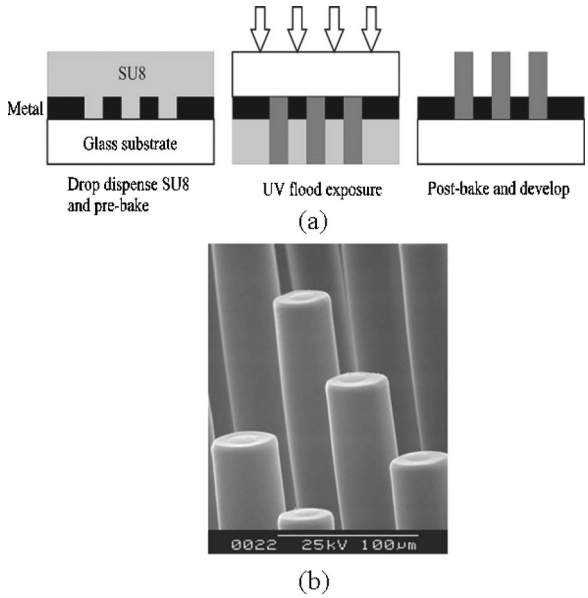

FIG. 1. SU8 pillar arrays, showing (a) fabrication flow on silicon substrates, and (b) final device realization.

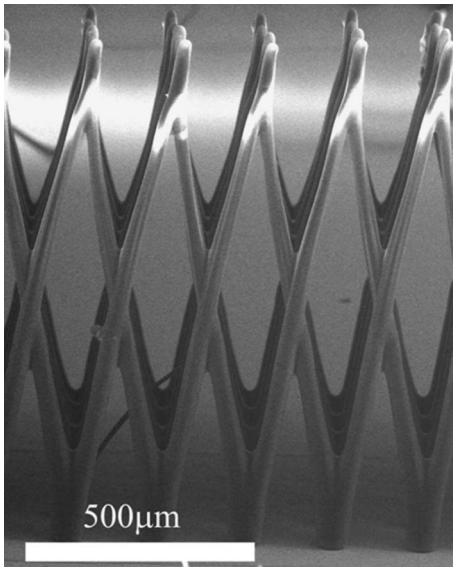

FIG. 2. A SU8 lattice fence structure fabricated by a variation on the process flow of Fig. 1.

FDTD and for complex photonic band structures analysis are then summarized briefly. The paper is concluded with a comparison between theory and experiment.

II. FABRICATION METHODS

The high aspect ratio (10:1 or greater) metal pillar arrays of the type used here, and illustrated in Fig. 1(b), are very challenging to fabricate using conventional micromachining techniques. Other groups have reported the use of microstereolithography[11] and x-ray exposure.[10] However, the more commercially viable ultraviolet (UV) micromachining approach has been overlooked until now. SU8 is a commercially available negative epoxy-based photoresist. When exposed to UV and thermally cured, it cross links and becomes both chemically and mechanically resistant. Conventional SU8 processing requires a separate mask which is brought into contact with the top of the soft baked resist during exposure. For very thick layers it is difficult to ensure that the SU8 at the bottom (which is in contact with the substrate) receives a sufficiently high dose of UV radiation. If the dose is too low then only partial cross linking occurs and the structures may delaminate during the wet development and release stages.

Figure 1 shows a self-masking approach which effectively solves the delamination problem. The SU8–50 is soft baked on a glass wafer which is coated with an optically opaque and patterned metal (in this case, gold). The resist is then drop dispensed and confined by an *O* ring during baking. After soft baking (5 h at 120 °C), the wafer can be flipped over and exposed with UV from the back. This is followed by post baking (1 h at 120 °C) and then the pillars are developed in EC-solvent (for approximately 18 h). Critically, this exposure technique ensures that the SU8 is well cross linked at the interface with the substrate. However, SU8 is transparent to THz and therefore, to complete the device, the pillars are sputter coated with gold (~0.3 μm) to produce structures of the type shown in Fig. 1(b). The exact thickness of the metal is not as important as that the process obtains a reasonably uniform coverage greater than the skin depth. The short mean free path between molecules in the sputtering process (no more than 3 mm at 10^{-2} Torr) ensures a nondirectionality to the metal coating and so a uniform deposition. The final structures are 1.3 mm tall. The process flow shown in Fig. 1 can produce a further type of high aspect ratio device through the use of angled UV exposure. Figure 2 shows a lattice structure formed using a double exposure at two different angles relative to the incident UV beam. Apart from the angled UV exposure, the fabrication process for lattice structures is identical to that for the high aspect ratio pillars. This includes a gold sputter coating to block the incident THz beam.

III. THZ MEASUREMENTS

THz time domain spectroscopy[6] (see Fig. 3) is used to measure the response of the artificial materials. A Ti:sapphire laser produces a 600 mW, near infrared (NIR) pulse of 20 fs duration with a repetition rate of 76 MHz. This is separated into THz-generating and detector-gating beams with a 70:30 beam splitter. The NIR generating beam is focused onto a GaAs photoconductive strip-line emitter, grown by molecular beam epitaxy, which is dc biased to 250 V. Parabolic mirrors are used to focus the THz signal onto the sample (spot size ~0.5 mm; and depth of field ~1.5 mm). The gating and the THz beam are focused onto a 1 mm thick zinc telluride electro-optic crystal. This, in conjunction with a balanced detector, is used to detect the THz radiation transmitted through the structure. A delay line on the NIR generation beam allows the electric field of the THz pulse to be scanned in the time domain. A fast fourier transform is then used to obtain a frequency spectrum. This system provides a usable bandwidth of approximately 3 THz. For relative transmission measurements, the sample scan is divided by a free space

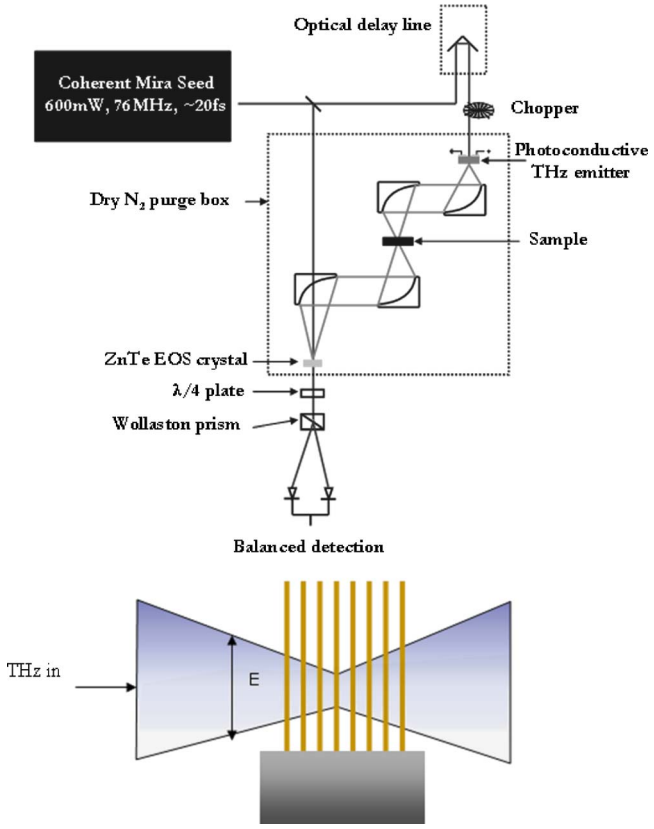

FIG. 3. (Upper) Experimental setup to investigate THz time domain spectroscopy showing the sample position. (Lower) The propagation direction of the THz beam relative to the vertical pillars.

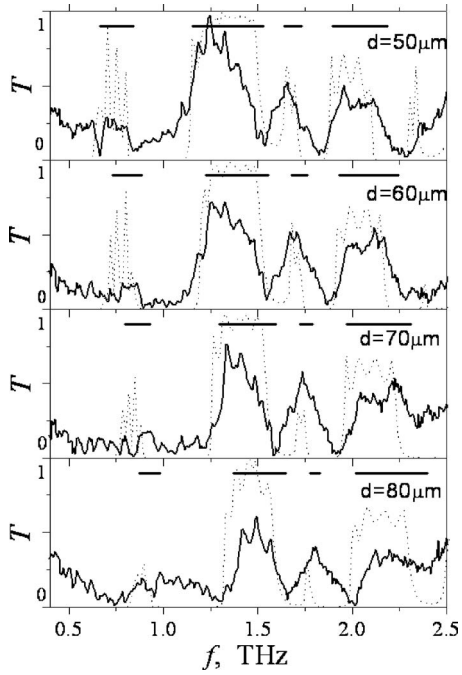

FIG. 4. Transmission of various pillar arrays. The pass bands, deduced from complex photonic band theory, are shown as dark horizontal lines. The "first band," referred to in the text, corresponds to the leftmost line; the "second" to the next band to the right; and so on. The dotted lines are FDTD simulations.

scan in the frequency domain. This effectively deconvolves any reflected signals associated with the measurement setup.

IV. TRANSMISSION OF METALLIZED PILLAR ARRAYS

In order to vary the characteristics of these filter structures, we fabricated devices with a range of pillar diameters but a constant period of 200 μm. This effectively changes the fill factor; it would be expected that (in addition to any frequency shift in the pass/stop bands) there would be a reduction in the relative transmission as the metal/air ratio increases in the filters. We have also fabricated pillar arrays, where we have varied the period between pillars both normal and parallel to the direction of the THz beam. Figure 4 shows the measured relative transmission for a six layer deep (in the direction of beam propagation) pillar array. The array is arranged in a square lattice, with the electric field component of the radiation orientated parallel to the pillar axes (see Fig. 3). The calculated transmission, with the pass band edges specifically marked, are also shown in Fig. 4. The calculations use FDTD simulations to generate the (dotted) transmission curves. The edges of the complex band structure edges are also shown. Further discussion is given in Sec. V. In each case the period is 200 μm; the pillar diameters vary from 50 μm to 80 μm; and the height of the pillars is 1.3 mm. The peak transmission for the pass bands is up to 97% with the stop bands at around 2%. Good correlation between theory and experiment is found. It is noted that the greatest transmission occurs for the second photonic band; this is a consequence of the plane wave radiation coupling less efficiently into the first band. It is also noted from Fig. 4 that, as the pillar diameter is increased, an increase in the center frequency of the main and secondary pass bands is observed. Furthermore, there is a reduction in the relative transmission, as would be expected.

These results show that the spectral shift associated with a relatively small (10 μm) increase in the pillar diameter is easily resolvable with the THz spectrometer set-up used here. This sensitivity to substantially highly subwavelength variations in the pillar diameter has a range of potential applications in sensing, in addition to that of THz filtering. Figure 5 shows the measured relative transmission characteristic from the six-layer deep lattice fence structure of Fig. 2. The maximum relative transmission is comparable to that of the 80 μm diameter pillar array in Fig. 4. However, the secondary pass bands shown in the pillar array case are more suppressed in the lattice device, leading to a single pass-band type transmission. While the THz transmission properties of the pillar array structures are amenable to theoretical analysis (see the next section), models to explain the properties of the "fence structures" are still under development.

V. THEORETICAL ANALYSES OF FILTER BEHAVIOR

Two approaches have been used to understand the behavior of the THz frequency filters: a complex photonic band structure technique[12] and FDTD simulations. However, before describing that work, it is appropriate to introduce the concept of an effective plasma frequency. Pendry *et al.*[8,9] studied the electromagnetic properties of thin wire structures,

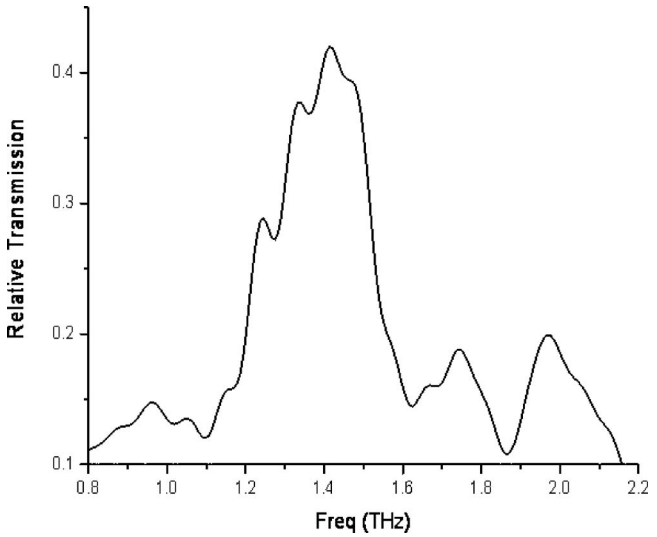

FIG. 5. Relative transmission for the lattice of Fig. 2.

essentially similar to the pillar forests considered here, and proposed a simple analytic theory to explain the principal feature characterizing their low frequency response to incident radiation: the existence of an effective plasma frequency below that of the bulk metallic value. In their thin wire model, which is notable for the fact that the result depends only on geometrical factors and not the bulk plasma frequency of the metal of the wires, the effective plasma frequency is given by

$$\omega_{p,\mathrm{eff}}^2 = \frac{2\pi c^2}{a^2 \ln(a/r)}, \tag{1}$$

where a is the lattice constant, r is the radius of the rods, and c the free-space velocity of light. In practice, no propagation can occur in the infinite structure below the effective plasma frequency, in analogy with the related effect in a homogeneous material. Since the work of Pendry *et al.*[8,9] a number of alternative simple analytic expressions for the effective plasma frequency have been proposed; further details are provided by Brand *et al.*[12] There have also been various other theoretical studies of both the photonic band structure for infinite systems[13,14] and the transmission properties in the case of finite structures.[15,16] Experimental results have been reported both in the original work of Pendry *et al.*[8,9] and also, more recently, by Pimenov and Loidl,[17] who investigated arrays of copper and steel wires using broadband THz spectroscopy. In their case, the experimental structures consisted of three rows of metal wires in a square grid with lattice period of about 0.5 mm. As a consequence of the larger lattice period, the frequency of interest in their study was rather lower than in the present work, about 0.2 THz.

Full details are given elsewhere[12] of the frequency dependent, plane wave based, complex band structure method that has been used here. In essence, the array of rods, shown in Fig. 6 is considered to be embedded in a medium with permittivity ε_b. The spatial dependence of the permittivity is then represented in the form

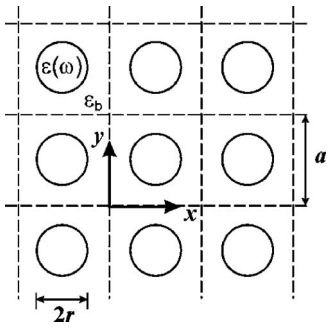

FIG. 6. An array of circular rods having a frequency-dependent relative permittivity $\varepsilon(\omega)$ embedded in a background material for which the relative permittivity has a constant value ε_b.

$$\varepsilon(x,y) = \varepsilon(\underline{\rho}) = \varepsilon_b + [\varepsilon(\omega) - \varepsilon_b] S(\underline{\rho}), \tag{2}$$

where $S(\underline{\rho})=1$ within the rods and $S(\underline{\rho})=0$ elsewhere. Using a Fourier-series expansion of $S(\underline{\rho})$ and the electric field within the structure, Maxwell's equations are solved. Knowing the form of $\varepsilon(\omega)$ it is possible to scan through frequency in order to determine the Bloch wave vector k, and thus the whole complex band structure of the system can be mapped out. For our calculations we take the background permittivity to be that of air, $\varepsilon_b=1$, and to represent the permittivity of the gold rods, we employ the Drude expression

$$\varepsilon(\omega) = 1 - \frac{\omega_p^2}{\omega(\omega + i\omega_c)}, \tag{3}$$

where numerical values $\omega_p = 2\pi \times 2.175 \times 10^{15}$ s^{-1} (for the bulk plasma frequency) and $\omega_c = 2\pi \times 6.5 \times 10^{12}$ s^{-1} (for the absorption term) are taken from Ordal *et al.*[19] The band structure calculations yield approximate values for the stop bands of the pillar array structures with a lattice constant of 200 μm, which are shown in Fig. 6 and in more detail in Fig. 7. In calculating these results the absorption term has been neglected without significant loss of accuracy. To obtain the results displayed in the figure, 877 plane waves were used for the electric field expansion. Other theoretical results, given elsewhere,[8,9] show how the effective plasma frequency

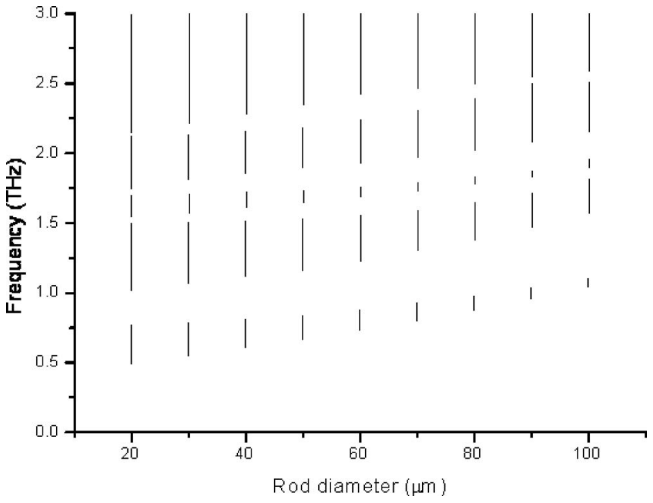

FIG. 7. The location of the first pass bands as function of rod diameter. The lowest band corresponds to the leftmost band in Fig. 4.

varies with the pillar diameter; a behavior which is best described by the simple analytical model of Maslovski *et al.*[18]

VI. CONCLUSION

We have designed, fabricated, and tested an artificial THz plasmonic material structure, a pillar forest, which may have applications as a system component at THz frequencies. We have demonstrated a readily available, UV based approach to the fabrication of this material. The process has been modified to include angled SU8 exposure which produces high aspect ratio lattice fence type structures. The pillar arrays fabricated using this technique showed a clear band structure in their THz transmission. The peak transmission of 97% makes this type of structure ideal for filtering or sensing applications. The effect of increasing the diameter of the pillars on the band structure is experimentally demonstrated and an increase in the center frequency of the main and secondary pass bands is observed. We have applied both an FDTD simulation and a photonic band gap analysis to model the transmission properties of these structures. The photonic band gap analysis provides an excellent description of the observed pass bands.

ACKNOWLEDGMENTS

The authors wish to acknowledge the support of the Engineering and Physical Science Research Council of the United Kingdom for funding (EP/C534263/1). They also wish to thank colleagues at Leeds University, U.K.; and, in particular, Edmund Linfield and Prasanth Upadhya, who provided the photoconductive emitter material used in this study as part of the UK Basic Technology Initiative.

[1] D. R. Smith, J. B. Pendry, and M. C. K. Wiltshire, Science **305**, 792 (2004).
[2] D. Schurig, J. J. Mock, B. J. Justice, S. A. Cummer, J. B. Pendry, A. F. Starr, and D. R. Smith, Science **314**, 977 (2006).
[3] K. Aydin and E. Ozbay, J. Opt. Soc. Am. B **23**, 415 (2006).
[4] J. M. Chamberlain, Philos. Trans. R. Soc. London, Ser. A **362**, 199 (2004).
[5] R. Kohler, A. Tredicucci, F. Beltram, H. E. Beere, E. H. Linfield, A. G. Davies, and D. A. Ritchie, Nature **417**, 156 (2002).
[6] D. M. Mittleman, M. Gupta, R. Neelamani, R. G. Baraniuk, J. V. Rudd, and M. Koch, Appl. Phys. B **68**, 1085 (1999).
[7] P. C. M. Planken and N. van der Valk, Opt. Lett. **29**, 2306 (2004).
[8] J. B. Pendry, A. J. Holden, W. J. Stewart, and I. Youngs, Phys. Rev. Lett. **76**, 4773 (1996).
[9] J. B. Pendry, A. J. Holden, D. J. Robbins, and W. J. Stewart, J. Phys.: Condens. Matter **10**, 4785 (1998).
[10] B. J. Shew, H. C. Li, C. L. Pan, and C. H. Ko, J. Phys. D **38**, 1097 (2005).
[11] D. M. Wu and N. Fang, Appl. Phys. Lett. **83**, 201 (2003).
[12] S. Brand, R. A. Abram, and R. A. Kaliteevski, Phys. Rev. B **75**, 035102 (2007).
[13] V. Kuzmiak, A. A. Maradudin, and F. Pincemin, Phys. Rev. B **23**, 16835 (1994).
[14] K. Sakoda, N. Kawai, T. Ito, A. Chutinan, S. Noda, T. Mitsuyu, and K. Hirao, Phys. Rev. B **64**, 045116 (2001).
[15] M. M. Sigalas, C. T. Chan, K. M. Ho, and C. M. Soukoulis, Phys. Rev. B **16**, 11744 (1995).
[16] P. Markos and C. M. Soukoulis, Opt. Lett. **28**, 846 (2003).
[17] A. Pimenov and A. Loidl, Phys. Rev. Lett. **96**, 063903 (2006).
[18] S. I. Maslovski, S. A. Tretyakov, and P. A. Belov, Microwave Opt. Technol. Lett. **35**, 47 (2002).
[19] M. A. Ordal, L. L. Long, R. J. Bell, R. R. Bell, R. W. Alexander, Jr., and C. A. Ward, Appl. Opt. **22**, 41099 (1983).